Solid Earth Discuss., 7, C1921–C1936, 2016
www.solid-earth-discuss.net/7/C1921/2016/

Solid Earth Discussions

Interactive comment on "Calculating structural and geometrical parameters by laboratory experiments and X-Ray microtomography: a comparative study applied to a limestone sample" *by* L. Luquot et al.

L. Luquot et al.

linda.luquot@idaea.csic.es

Received and published: 4 February 2016

Dear Reviewer 2,

First we would like to thank the anonymous reviewer 2 for his/her comments and his/her interest in our article to be published in Solid Earth. Please find below and in the revised manuscript the answers and comments for each specific reviewer question/comment.

Specific comments

1. P. 12, l. 4: Gx is the gray level of a voxel belonging to the subresolved porous phase. We modified the sentence at p. 12, l. 2-3 as follows: "The gray level value Gx of a voxel belonging to the subresolved porous phase is linearly related to φx as follows:"

2. P. 12, on "Evaluating errors in porosity calculation"

We would like to thank the reviewer for this comment as the thresholding step is the most important in the CT process. Consequently, evaluating its error on structural and geometrical parameters is essential. Usually, based on the gray scale histogram, one can determine the pretended "best" threshold value. Nevertheless, it is known that this value n used for thresholding is relative/conditional to the user. So after determining the "optimal" threshold value based on the histogram (added now in the new manuscript, see comment no. 4), we decided to perform four more segmentation steps increasing and decreasing by 1 and 2 the initial selected threshold value n. Afterwards we evaluated the thresholding error comparing the porosity values obtained for the different thresholding values. In order to be more clear-cut, we inserted the following sentence at l. 8: "For instance, if an image is segmented using a basic thresholding technique, then one can perform extra segmentations by varying threshold values by one or two units and computing the associated porosities."

3. P. 15, l. 16

Comparing the calculated chemical porosity after the dissolution experiment by the mass balance method and the one evaluated by XMT images, we calculated a pore volume difference of 90 mm3, which is less than 1% of the total core volume. This difference is less than the possible error of porosity calculation due to the thresholding step (see comment no. 2) and can consequently be an explication of the porosity difference. Nevertheless, as initially only 37.80% of the resolved phase volume was connected, one can expect that the dissolution process allows connection of "closed" pores as the final resolved phase is connected more than 93%. So in order to compare the porosity difference obtained by mass balance and the one computed in the XMT

images, we measured the volume of non-connected pores initially presented in the final wormhole feature. We measured a non-connected pore volume equal to 32 mm3. Knowing that the dissolution process is mainly localized but not exclusively, the initially non-connected pore volume only in the final wormhole feature is clearly underestimated but indicate that the hypothesis of the connection of initial non-connected pore by the dissolution process can explain the porosities difference is more than reasonable. To illustrate this phenomenon, we add the new figure 12. This new figure allows also to illustrate more the core structure and the use of XMT images as commented as a general comment by the reviewer.

4. P. 18, l. 14-20

We totally agree with the reviewer comment. It is true that the histogram feature and the localization of the threshold value is a key parameter to discuss on the accuracy of the results. To be more specific, we added the new Figure 1 where we can observe the histogram shape corresponding to Bvl before dissolution experiment. The n value selected for the threshold is indicated in the figure. In general, thresholds are not supposed to be chosen among the values having the highest intensities. However, the slope of the tangent at the value where it is chosen is indeed determinant, as the choice of different but close thresholds amongst values of similar frequencies can yield to assigning many pixels to one phase or another. This is why performing different segmentations with close thresholds can give very different results, especially in this particular case.

5. P. 19, l. 13

We don't really understand the comment. If is the point is to know if other authors already visualized wormhole formation in core samples using XMT images, the answer is yes. We can cite for example Luquot and Gouze (2009); Ellis et al (2011) ; Luquot et al, (2014); Tutolo et al (2014); Menke et al (2015); Noiriel (2015) among others. What we claim here is that without the 3D images, the porosity profiles and other parameters

can not be used to prove the wormhole formation as in other cases, similar porosity change trends were characterized for homogeneous dissolution process.

6. We modified Figure 8 (now Figure 9) as suggested by the reviewer in order to be more understandable.

7. P. 24, l. 10-15

Actually, we mentioned that using this technique it is possible to extract the throat distribution as well as the pore distribution. Nevertheless, for this article, we just calculated the pore size distribution. The throat definition is still an open discussion to which we expect to contribute soon.

General comments

We added another 3D image as suggested by the reviewer and a 2D image extracted from the 3D one to better observe the rock structure. See comments no. 3 and Figures 1 and 12.

Please also note the supplement to this comment:
http://www.solid-earth-discuss.net/7/C1921/2016/sed-7-C1921-2016-supplement.pdf

---

Interactive comment on Solid Earth Discuss., 7, 3293, 2015.

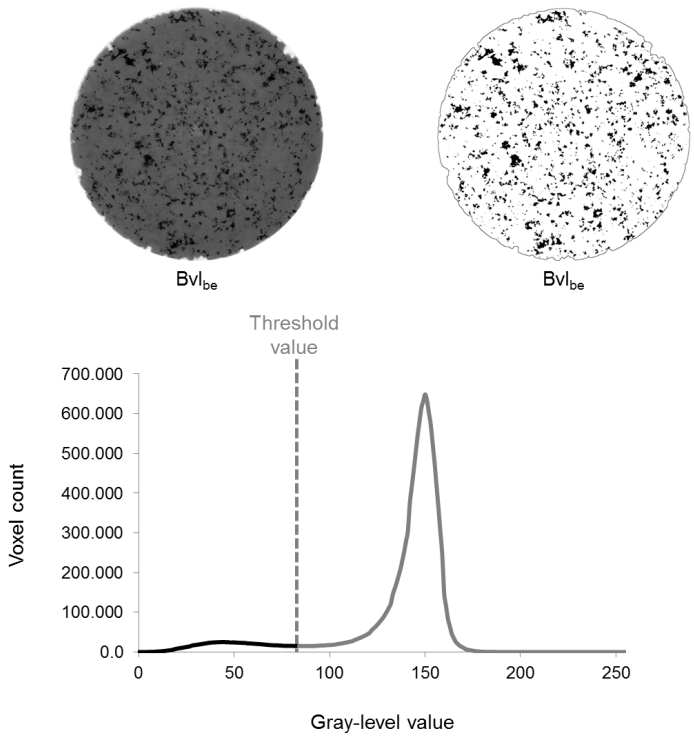
BvI_{be}
BvI_{be}
Threshold value
700.000
600.000
500.000
400.000
300.000
200.000
100.000
0.0
Voxel count
0
50
100
150
200
250
Gray-level value

Fig. 1.

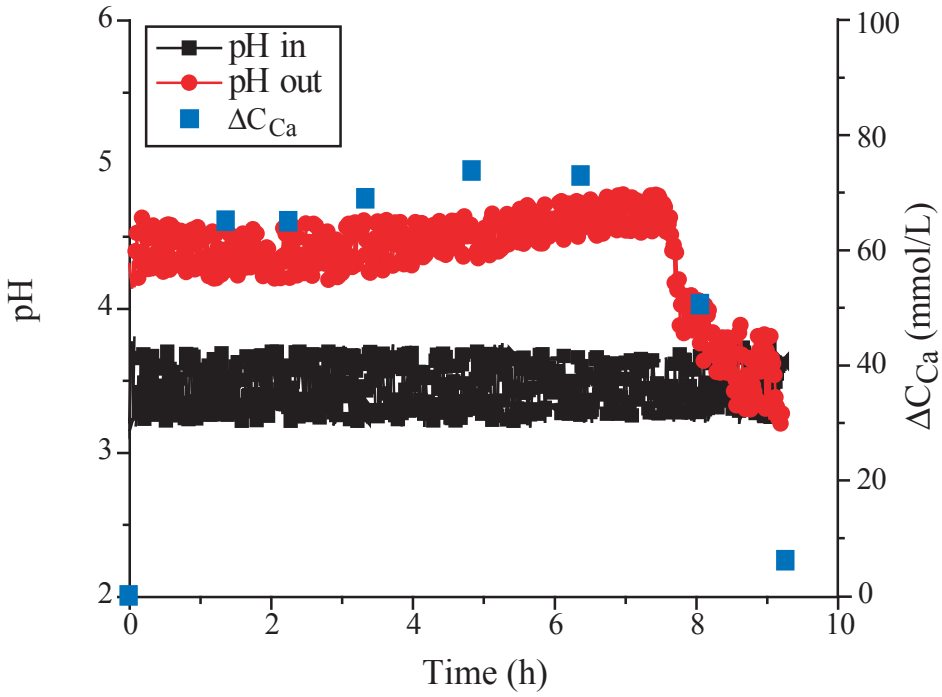
pH in
pH out
ΔC_{Ca}
pH
ΔC_{Ca} (mmol/L)
Time (h)
2
3
4
5
6
0
20
40
60
80
100
0
2
4
6
8
10

Fig. 2.

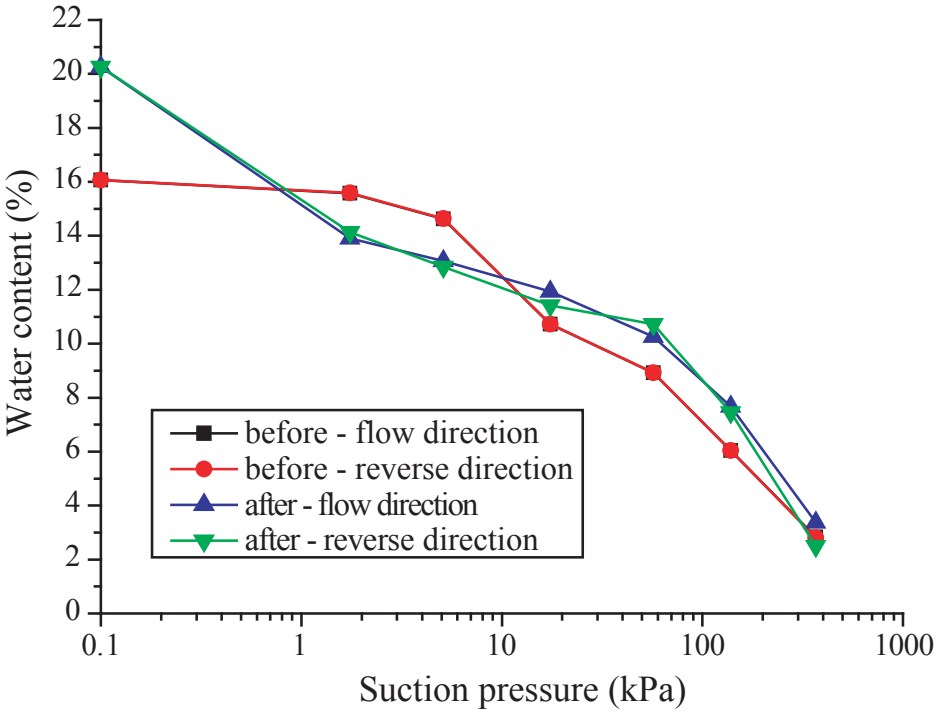
Water content (%)
Suction pressure (kPa)
before - flow direction
before - reverse direction
after - flow direction
after - reverse direction

Fig. 3.

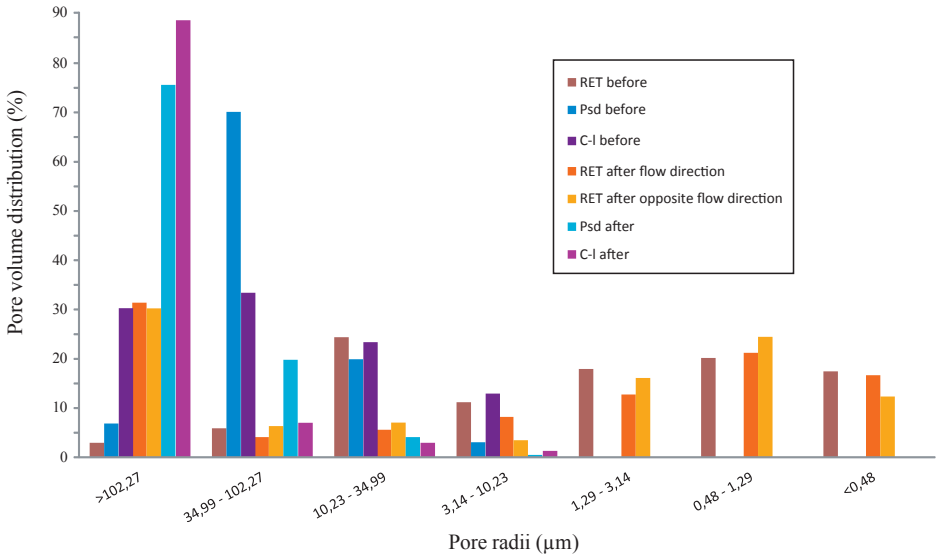
Pore volume distribution (%)
Pore radii (µm)
RET before
Psd before
C-l before
RET after flow direction
RET after opposite flow direction
Psd after
C-l after
>102,27
34,99 - 102,27
10,23 - 34,99
3,14 - 10,23
1,29 - 3,14
0,48 - 1,29
<0,48

Fig. 4.

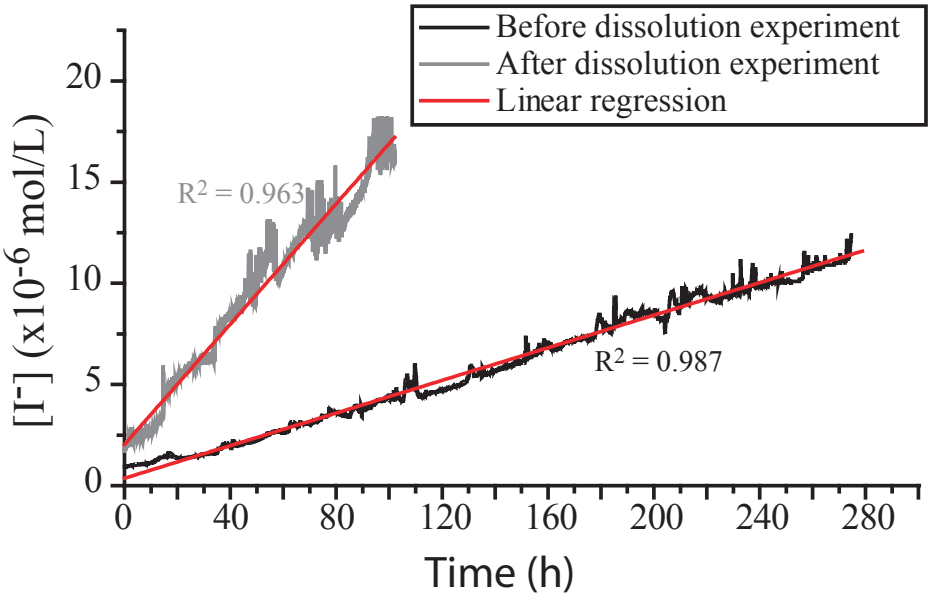
Before dissolution experiment
After dissolution experiment
Linear regression
R2 = 0.963
R2 = 0.987
[I-] (x10-6 mol/L)
Time (h)
0
5
10
15
20
0
40
80
120
160
200
240
280

Fig. 5.

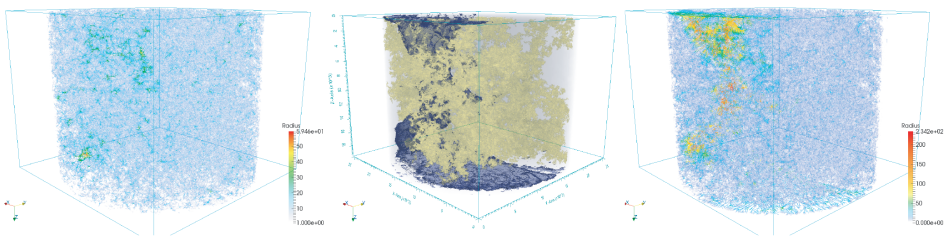

Fig. 6.

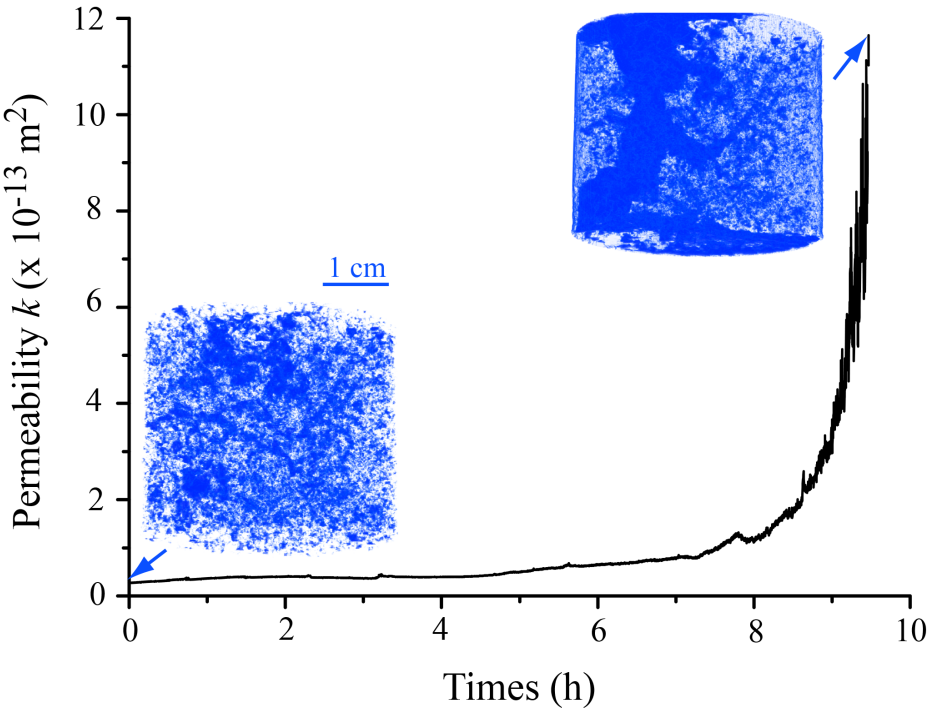
Permeability k (x 10^{-13} m^2)
Times (h)
1 cm
0
2
4
6
8
10
12

Fig. 7.

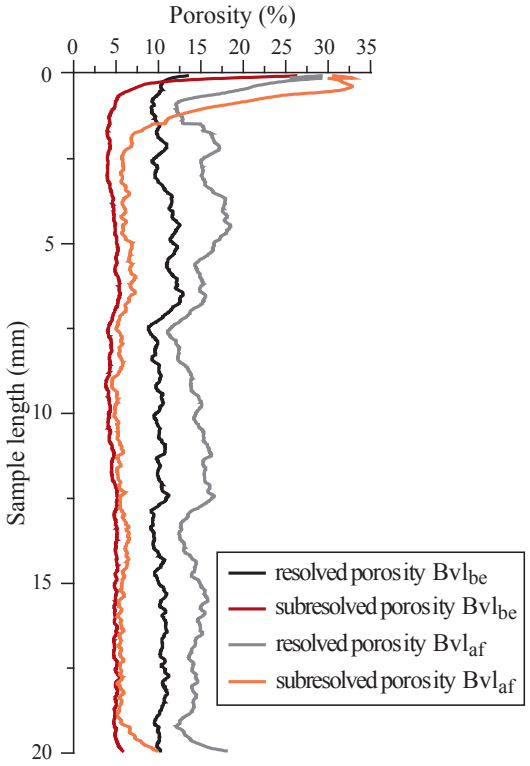
Porosity (%)
Sample length (mm)
resolved porosity Bvl_{be}
subresolved porosity Bvl_{be}
resolved porosity Bvl_{af}
subresolved porosity Bvl_{af}

Fig. 8.

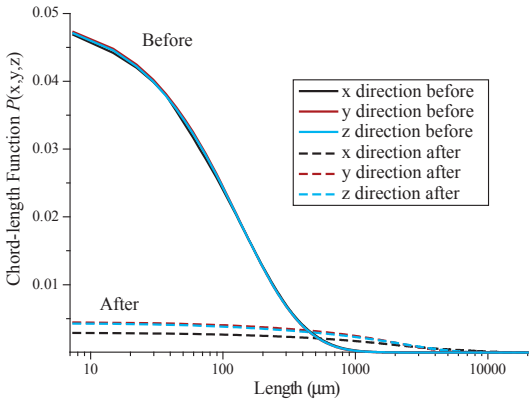
Before
After
x direction before
y direction before
z direction before
x direction after
y direction after
z direction after
Chord-length Function P(x,y,z)
Length (μm)
0.05
0.04
0.03
0.02
0.01
10
100
1000
10000

Fig. 9.

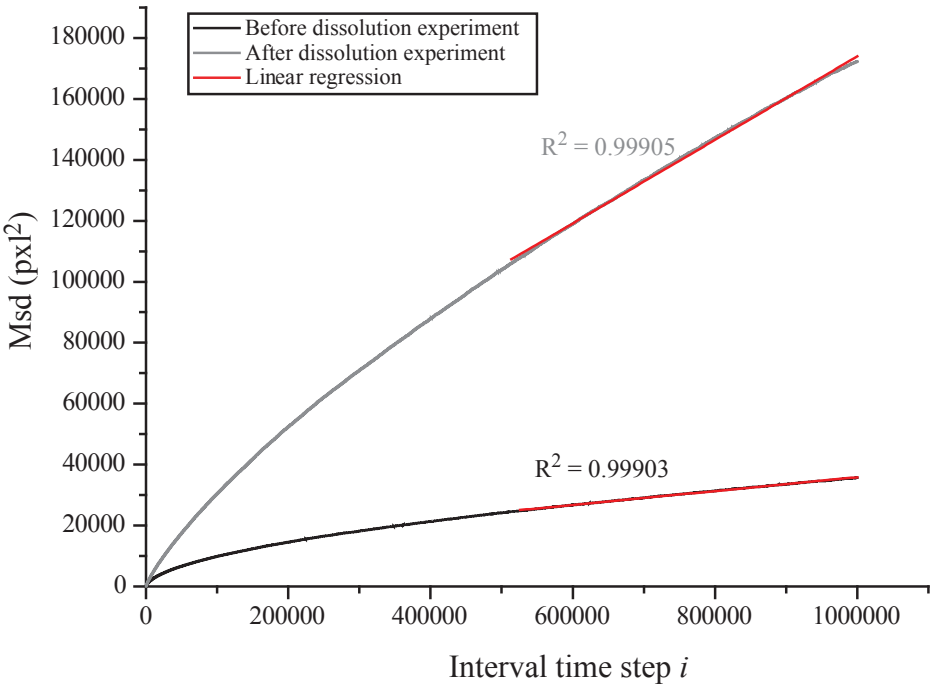
Before dissolution experiment
After dissolution experiment
Linear regression
R2 = 0.99905
R2 = 0.99903
Msd (pxl2)
Interval time step i
180000
160000
140000
120000
100000
80000
60000
40000
20000
0
0
200000
400000
600000
800000
1000000

Fig. 10.

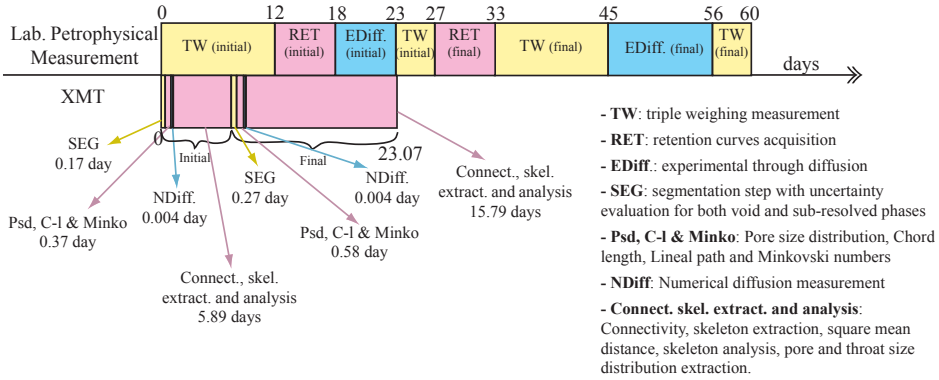
0
12
18
23
27
33
45
56
60
Lab. Petrophysical Measurement
TW (initial)
RET (initial)
EDiff. (initial)
TW (initial)
RET (final)
TW (final)
EDiff. (final)
TW (final)
days
XMT
0
23.07
Initial
Final
SEG 0.17 day
NDiff. 0.004 day
SEG 0.27 day
NDiff. 0.004 day
Connect., skel. extract. and analysis 15.79 days
Psd, C-l & Minko 0.37 day
Connect., skel. extract. and analysis 5.89 days
Psd, C-l & Minko 0.58 day
- TW: triple weighing measurement
- RET: retention curves acquisition
- EDiff.: experimental through diffusion
- SEG: segmentation step with uncertainty evaluation for both void and sub-resolved phases
- Psd, C-l & Minko: Pore size distribution, Chord length, Lineal path and Minkovski numbers
- NDiff: Numerical diffusion measurement
- Connect. skel. extract. and analysis: Connectivity, skeleton extraction, square mean distance, skeleton analysis, pore and throat size distribution extraction.

Fig. 11.

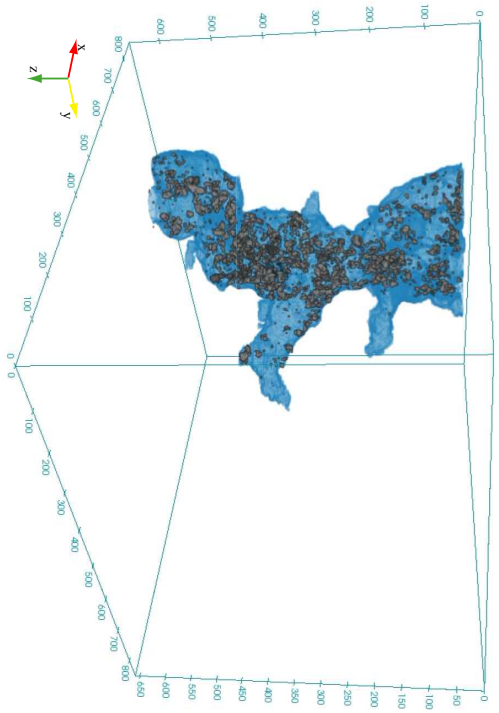
x
z
y

Fig. 12.